J Fluoresc (2012) 22:1563–1569
DOI 10.1007/s10895-012-1096-3

ORIGINAL PAPER

UV-Visible Photoluminescence of TiO_2 Nanoparticles Prepared by Hydrothermal Method

S. Mathew · Amit Kumar Prasad · Thomas Benoy · P. P. Rakesh · Misha Hari · T. M Libish · P. Radhakrishnan · V. P. N. Nampoori · C. P. G. Vallabhan

Received: 8 February 2012 / Accepted: 20 June 2012 / Published online: 5 July 2012

Abstract TiO_2 colloidal nanoparticles and nanocrystals are prepared by hydrolysis of titanium isopropoxide employing a surfactant-free synthetic hydrothermal method. The synthesized samples are characterized by X-ray diffraction (XRD), HRTEM and FTIR. The XRD study confirms that the size of the colloidal nanoparticle is around 4 nm which the HRTEM analysis indicates the sizes of the colloidal nanoparticles are in the range of 2.5 nm. The fluorescence property of the TiO_2 colloidal nanoparticles studied by the emission spectrum confirms the presence of defect levels caused by the oxygen vacancies. We have observed new emission bands at 387 nm,421 nm, 485 nm, 530 nm and 574 nm wavelengths, first one (387 nm) being emission due to annihilation of excitons while remaining four could be arising from surface states. The emission spectrum of annealed nanocrystallites is also having these four band emissions. It is observed that the surface state emission basically consists of two categories of emission.

Keywords Colloidal nanoparticles · Anatase · Fluorescence

Introduction

Scientific investigations on nanocrystals, quantum dots, quantum well, and atomic and molecular clusters have grown dramatically over the past decade. A general approach in these fields is to study the optical properties of a given substance as a function of size and dimensionality. When the characteristic size of the particles is comparable or smaller than its bulk Bohr exciton diameter, its optical properties become strongly dependent on size due to the quantum confinement of electrons and holes [1–5]. Recently, intense efforts have been made to develop metal oxide semiconductor materials with typical optical properties such as strong photoluminescence, electroluminescence, or nonlinear optical behaviour, which may lead to new optoelectronic devices with superior performance [6, 7]. Besides, optical studies can give sufficient information about energy level structure of these materials. Titanium dioxide in this context is one of the well-studied transition metal oxides. TiO_2 is a very interesting UV absorbing material not only from a scientific standpoint but also due to its technological applications in dye sensitized solar cells, pigments , dielectric materials in capacitors, and so on[8–10]. At ambient pressure TiO_2 is known to exist in three polymorphs: rutile, anatase and brookite. Anatase and rutile are the two main crystalline phase structures of TiO_2 with band energies at 3.2 eV and 3.0 eV respectively. As an n-type semiconductor with a wide energy band gap, TiO_2 is also well-known for its potential applications in the field of photocatalysis and photo electrochemistry because of its excellent optical transmittance, high refractive index and chemical stability. In addition to quantum confinement effects, semiconductor nanoclusters show properties that are strongly affected by their large surface-to-volume ratios. Recently, efforts have been directed to obtain nanostructured TiO_2-based materials with a large specific surface area. The energy band structure becomes discrete for TiO_2 at nanometer scale, and its photo physical, photochemical, and surface properties are quite different from those of the bulk due to the quantum size effect. A significant fraction of the atoms resides on the

S. Mathew (✉) · M. Hari · T. M. Libish · P. Radhakrishnan · V. P. N. Nampoori · C. P. G. Vallabhan
International School of Photonics, CUSAT,
Kochi, India
e-mail: mathewphys@gmail.com

S. Mathew · A. Kumar Prasad · T. Benoy · P. P. Rakesh · P. Radhakrishnan
Center of Excellence in Lasers and Opto electronic Sciences
CUSAT,
Kochi, India

nanocluster surface and these surface atoms have "dangling bonds" which may act as electron/hole traps that can dominate electron–hole recombination and other processes. This process will yield a significant emission and those are regarded as surface state emission [11]. In TiO_2, it is difficult to observe band edge luminescence. But the relationship of the photoluminescence arising from features with the crystal structures of TiO_2 is yet to be investigated. The optical properties of nanocrystalline TiO_2 have been tentatively studied in recent years and many interesting results have been obtained [12–14].

Although TiO_2 nanoparticles are considered to be one of the most important quantum semiconductor particles, there are only a few reports that describe the preparation of crystalline TiO_2 nanoparticles monodispersed in a stable suspension. The preparation of TiO_2 nanoparticles in solution phase would be one of the best synthetic routes, both for controlling the size of individual particles and for obtaining the stabilized colloidal suspensions. The suspended crystalline nanoparticles not only serve as ideal precursors for further material development but also offer some other unique opportunities, such as enabling studies of their optical, photocatalytic and other fundamental properties under solution-like conditions. The optical properties of these suspended nanoparticles have not been studied in great detail [15–18]. Time-resolved photoluminescence spectroscopy studies by Xiuli Wang et.al gives an insight into the distribution of trap states and their effect on carrier dynamics in TiO_2[19]. In the present study, we report the optical properties of TiO_2 colloidal nanoparticles and nanocrystallites with emphasis to fluorescence spectra.

Experimental

TiO_2 colloidal nanoparticles were prepared by hydrolyzing titanium isopropoxide. The materials used for the preparation of colloidal TiO_2 are: titanium (IV) isopropoxide (TIP, $Ti(C_3H_7O)_4$) used as titanium precursor, nitric acid (HNO_3) as peptizing agent, deionized water and isopropanol (C_3H_7OH) as solvent. Titanium (IV) isopropoxide of synthesis grade purchased from Lancaster. All the other chemicals are of GR grade from Merck Ltd

In this work, we stabilized titanium isopropoxide in acidic isopropanol / water solution prior to hydrothermal reaction. The precursor solutions is made by mixing varying volume percent of titanium isopropoxide(TIP (97 %)) as 0.5 %, 0.9 %, 1.1 %, 1.4 % and 2.9 %, 15 ml of Isopropanol and 250 ml solution of distilled water with varied pH obtained by adding HNO_3. These solutions are vigorously stirred and annealed at 60 °C for 8 h and this gives white bluish stable TiO_2 colloidal nanoparticles as a result of the thermal decomposition of TIP are termed as T1(0.5 %), T2(0.9 %), T3(1.1 %), T4 (1.4 %)and T5(2.9 %) samples. These colloidal nanoparticles are optically characterized by measurement of their light absorption at room temperature which is carried out using a spectrophotometer (JascoV-570 UV/VIS/IR). The fluorescence emission from the same sample was recorded using a Cary Eclipse fluorescence spectrophotometer (Varian). TiO_2 colloidal nanoparticles (T4) are dried and annealed at 400 °C to get yellowish white nanocrystallite. These nanocrystals were also optically characterized as mentioned in the case of TiO_2 colloidal nanoparticles. The Fourier transform infrared (FT-IR) spectra of the samples were collected using Thermo Nicolet, Avatar 370 infrared spectrometer. The structural properties of this sample are investigated by X-ray diffraction (XRD) on a Bruker AXS D8 Advance x-ray diffractometer with Ni-filtered Cu $K\alpha$ (1.5406 Å) source ll. Transmission electron microscopy (SEM) of TiO_2 colloidal nanoparticles and annealed nanocrystals were performed on JOEL HRTEM machine for size measurement

Results and Discussions

Figure 1(a) show the UV–VIS absorption spectra recorded for TiO_2 colloidal nanoparticles. Absorption edge is blue shifted as the concentration of the precursor is reduced. Similar observations have been made during the case of ZnO nanoparticles in colloidal solution and were interpreted in terms of quantum confinement effects [20, 21]. This is termed as Q size effects. i.e., the particle size is reduced when the concentration is reduced. Titania possesses a highly ionic lattice with the valence band composed principally of oxygen 2p orbitals, with the corresponding wave functions considerably localized on the O^{2-} lattice sites. The conduction band consists mostly of excited states of Ti^{4+}.

In order to determine the nature of the optical band gap as either indirect or direct, one has to consider the variation of the absorption coefficient with energy. Bulk TiO_2 is an indirect band gap semiconductor. In this case a two-step process is necessary for the optical transition because a photon cannot provide the required change in momentum and the lowest-energy inter-band transition must then be accompanied by phonon excitation. When phonon energy can be neglected, the absorption coefficient α near the absorption edge for indirect inter-band transitions is given by Eq. 1 [22]. Indirect inter-band transitions are characterized by the stronger energy dependence of the optical absorption coefficient nearer the absorption edge than is otherwise as in the case for direct transition

$$\propto = B_i(h\vartheta - E_g)^2/h\vartheta \quad (1)$$

where B_i is the absorption constant for an indirect transition.

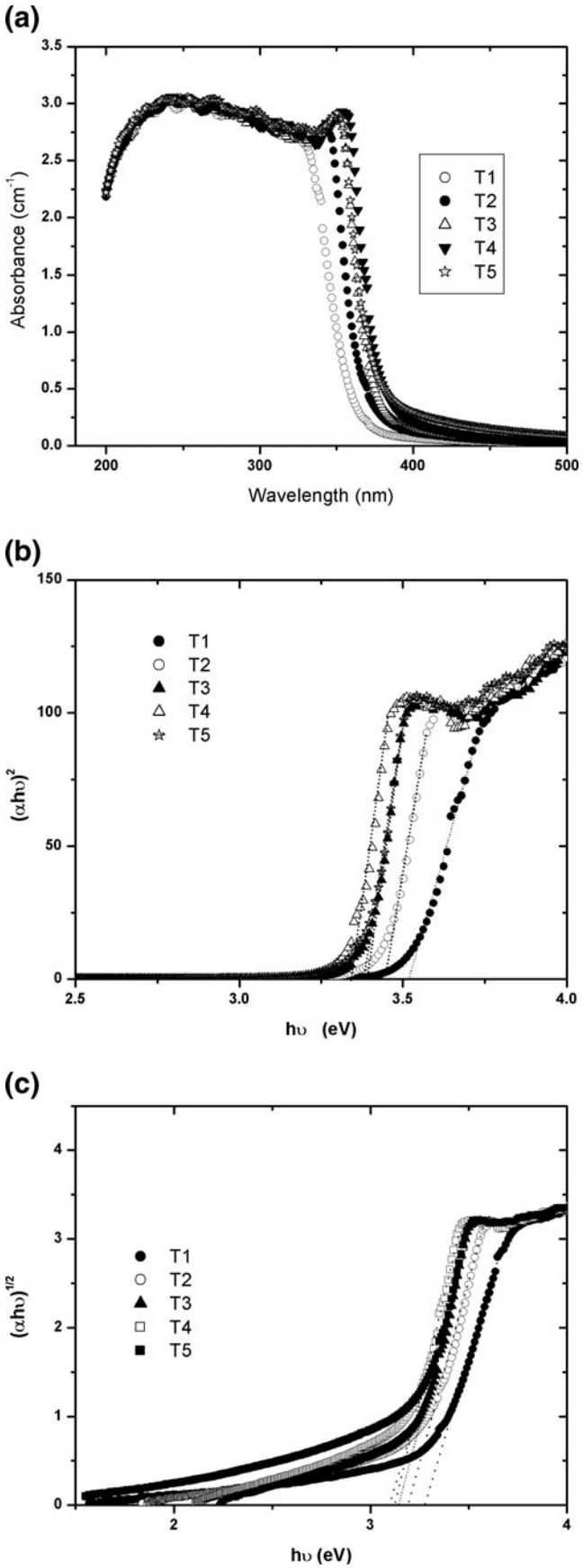

Fig. 1 **a**: Absorption spectra of colloidal TiO_2 particles, (**b**): Direct optical band gap transitions$(\alpha h\upsilon)^2$ vs hυ plot, (**c**): Indirect optical band gap transitions $(\alpha h\upsilon)^{1/2}$ vs hυ plot

Serpone et al. [15] have established that both indirect and direct transition mechanisms are operative in nanophase TiO_2. In the case of direct band gap semiconductor, the optical absorption coefficient near the absorption edge for inter-band transitions is given by Eq. 2

$$\propto = B_d(h\vartheta - E_g)^{1/2}/h\vartheta \tag{2}$$

where B_d is the absorption constant for a direct transition

In our case, the spectrum is characterized by a sharp band edge along with a series of exciton states. Figure 1(b) and (c) represent direct and indirect optical band gap plots for T1, T2, T3, T4 and T5 colloidal nanoparticles. The direct band gap of these colloidal nanoparticles are obtained by plotting $(\alpha h\upsilon)^2$ versus hυ graph, shown in Fig. 1(b). The band gap of colloidal nanoparticles gets decreased, when the precursor concentration is increased. From Fig. 1(b), the estimated direct band gap of T1, T2, T3, T4 and T5 are 3.52 eV, 3.45 eV, 3.39 eV, 3.34 eV and 3.38 eV. Thus a direct band gap variation of 0.18 eV can be obtained by varying the precursor concentrations and these could be attributed to the $X_1 \rightarrow X_1$ transitions. In the case of indirect direct transitions, Fig. 2(b) shows intercepts at 3.28 eV, 3.2 eV, 3.15 eV, 3.12 eV and 3.19 eV which are the indirect band gaps which are somewhat red-shifted as the concentration of the precursor is increased (a band gap tuning of around 0.16 eV) and it is assigned to $\Gamma_1 \rightarrow X_1$ transitions, where X denotes the edge and Γ the centre of the Brillouin zone [23].

It is observed that the absorption of colloidal nanoparticles is higher than that of annealed sample. The absorption

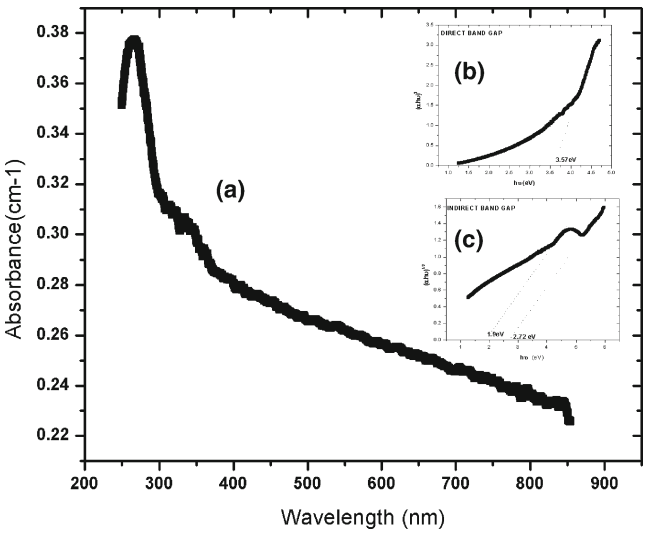

Fig. 2 **a** Absorption spectra of annealed TiO_2 nanocrystals, insets (**b**) $(\alpha h\upsilon)^2$ vs hυ plot and (**c**) $(\alpha h\upsilon)^{1/2}$ vs hυ plot

spectrum of the annealed TiO_2 nanoparticles is shown in Fig. 2(a). Figure 2(b), (c) represents the direct and indirect band gaps for the annealed sample. The extrapolated intercept occurs at 2.72 eV which can be assigned to the indirect transition (Fig. (2c)) for the annealed sample. The inset in Fig. 2(b) represents the direct band gap plot and it is found that the value of band gap 3.57 eV ($X_2 \rightarrow X_1$ transition) [24]. This can be explained due to the reduced ionicity of the TiO_2 phase synthesized, which results from mixing of the O^{2-} p-orbitals and T_i^{3+} d- orbitals. Similar absorption features have been seen in the work of Serpone et al. [15].

Figure 3 shows the FTIR spectrum of the TiO_2 samples prepared as described earlier. From this spectrum, it can be observed that strong band in the range of 880 and 450 cm^{-1} is apparently associated with the characteristic vibrational modes of TiO_2. The absorption at 3391 cm^{-1} indicates the presence of hydroxyl group, which is probably due to the fact that the spectra were not recorded in situ and some readsorption of water from the ambient atmosphere has occurred [24]. In this figure, strong bands at 3,400 and 1,630 cm^{-1}, which are attributed to the stretching mode of the –OH group and the deformation mode of molecular water respectively, can be seen.

Figure 4 shows the XRD pattern of (a) colloidal nanoparticles and (b) annealed particles. The XRD pattern of colloidal particles shows broad peaks compared to that of annealed particles. The broadness of peaks indicates that the colloidal particles are much lower in size compared to annealed particles. All the diffraction lines are assigned well to anatase crystalline phase of titanium dioxide except a small peak at 30.65°. The separate peak at 30.65° indicates the presence of brookite phase of TiO_2. The diffraction peaks of (101), (004), (200), (105)) correspond to the anatase TiO_2 phase. The separate peak at (121) assigned to the XRD pattern is in excellent agreement with a reference

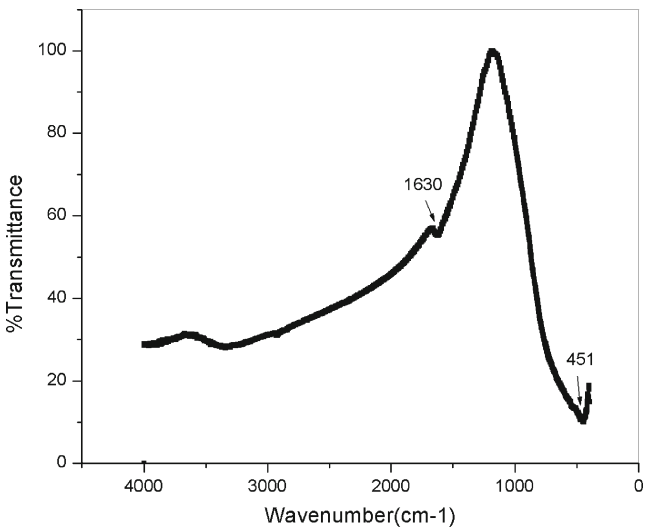

Fig. 3 FTIR spectrum of TiO_2 nanocrystals

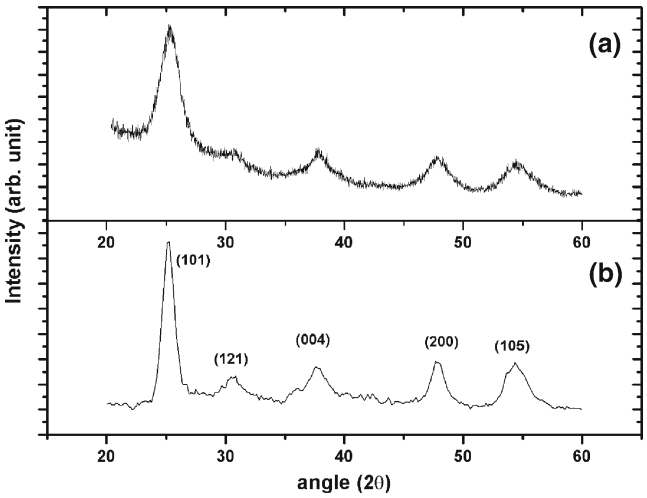

Fig. 4 Xrd spectra of TiO_2 nanoparticles and annealed TiO_2 nanocrystals

pattern (JCPDS 21-1272) of titanium dioxide. It should be noted that only anatase TiO_2 can be detected and no rutile phase can be found in this sample, which can be attributed to the contribution of the low concentration of oxygen vacancies due to the high concentration of gaseous oxygen during particle growth, hindering the transformation from anatase to rutile phase. It is noted that the particle size plays an important role in deciding the crystal structure. Using Debye–Scherrer's formula ($[D = 0.89\lambda/\beta\cos(\theta)]$, where D is the particle diameter, λ is the wavelength of x-ray used, β is the full width half maximum and θ is the scattering angle), the estimated particle size for the colloidal particles is in the range of 4 nm, and for the annealed particles the estimated size is found to be around 8 nm. i.e., sample while annealed at 400 °C yields much larger particles compared to the non-annealed sample. This is due to the aggregation of particles while annealing the colloidal nanoparticles.

The Transmission electron micrographs (HRTEM) of T_4 colloidal particles are shown in Fig. 5. It shows that the particles are having spherical shape and the size of the particles is found out to be around 2.5 nm and also shows the d-spacing of the colloidal particles around 3.62°A which is agreement with the literature value. This is slightly less than the size of particle from X-ray diffraction analysis.

The optical properties of a semiconductor are mainly determined by its electronic structure, so the essence of light absorption will be found by studying the relationship between electronic structure and optical properties of TiO_2. After excitation by photon, the electron–hole pairs might recombine in the process of migration from inside to the surface of the crystal. The recombination rate is closely related to the electronic structure and crystal structure. As TiO_2 has a broadband absorption, excitation spectrum is very significant in finding the excitation wavelengths at which it has maximum emissions. Figure 6(a) shows the

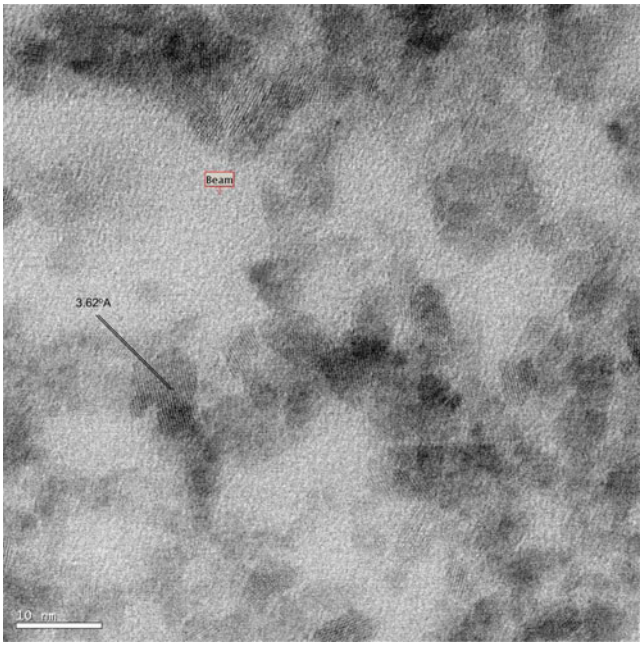

Fig. 5 TEM picture of colloidal (T3) TiO_2 nanoparticles

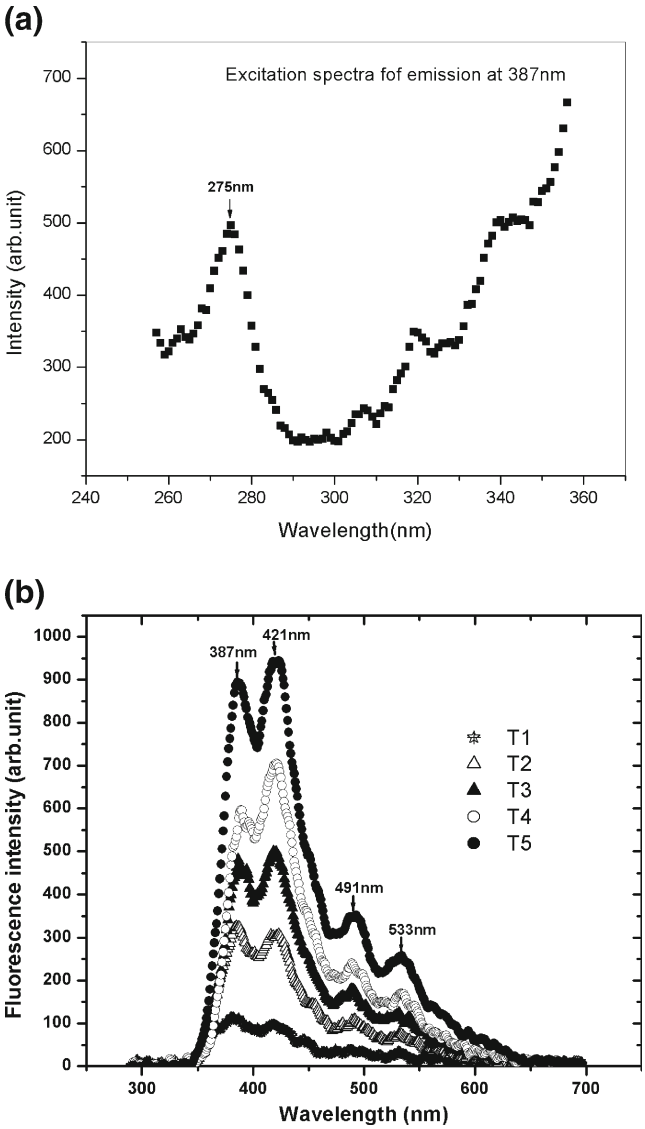

Fig. 6 **a**: Excitation spectra of TiO_2colloidal nanoparticles. **b**: Fluorescence spectrum of colloidal nanoparticles

excitation spectrum for emission peak of 387 nm. From the absorption spectrum it is clear that the peak wavelength 274 nm of excitation spectrum is coming in the high absorption range. Figure 6(b) shows the fluorescence spectrum of the TiO_2 colloidal nanoparticles (T1, T2, T3, T4 and T5) for the excitation wavelength of 274 nm. From the fluorescence spectrum, emissions at 387 nm, 421 nm, 491 nm and 533 nm are observed. These emission peaks occurring at larger wavelengths with respect to the band edge emission (387 nm) are attributed to the quasi-free recombination at the absorption band edge, the shallow- trap state near the absorption band edge, the deep-trap band far below the band edge, and a combination of these effects, are called the surface state emissions. Surface state is generally localized within the band gap of the semiconductor and they can trap the excited state electrons and lead to higher wavelength emissions. The quasi free recombination and shallow trap emission could be overlapping due to broad size distribution as there is no capping agent is used in this preparation. The oxygen vacancies and surface hydroxyl groups are dominant sites for trapped electrons and holes. These trapped carriers which are captured by oxygen vacancies and surface hydroxyl groups, contribute to the visible luminescence in these nanoparticles. Emission at 387 nm is found to be excitonic emission. 421 nm, 491 nm, 533 nm emissions are assigned to the surface state emissions and are due to the recombination of trapped electron–hole arising from dangling bonds in the TiO_2 nanoparticles. Figure 7 shows the fluorescence spectrum of the annealed sample, the intensity of emission peak at 422 nm is higher than that of 387 nm which indicates that the nanoparticle having more surface states dominate the excitonic emission. Other emissions around 493 nm, 534 nm and 573 nm are having less intensity compared to the peaks at 421 nm and 387 nm. The emission at 534 nm is found to be due to O^{2-} vacancies. In this case the photoluminescence is mostly a surface phenomenon, and a change in the surface environment would have a significant effect on the photoluminescence process. Therefore, it is concluded that the visible luminescence band originates from the oxygen vacancies associated with Ti^{3+} in anatase TiO_2. Similar description of the visible luminescence band was reported earlier [18, 25, 26]. The whole emission mechanism is depicted in the Fig. 8.

It is observed that the surface state emission basically consists of two categories of emission. One set occurs as series giving emissions at 421 nm, 491 nm and 573 nm with almost a difference of nearly 80 nm. This set of emissions is

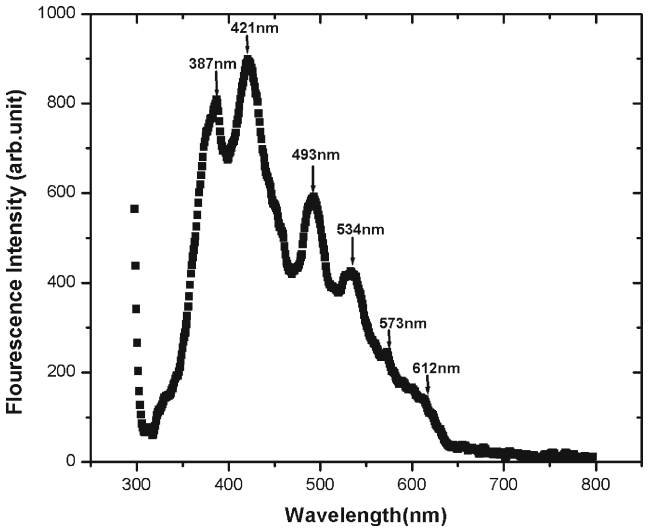

Fig. 7 Fluorescence spectrum of annealed TiO_2 nanocrystals

from the deexcitation from lower vibronic levels in Ti^{3+} 3d states of TiO_2 lattice to the deep trap levels (acceptor) created by (OH-). And other set is having emission wavelengths 533 nm and 612 nm, which are also separated by nearly 80 nm. These emissions are due to deexcitation from lower vibronic levels in deexcitation from lower vibronic levels in the oxygen vacancies of TiO_2 lattice to the ground state.

In order to find out dependence of the increase in particle size of colloidal TiO_2 nanoparticles on the excitonic and surface state emission, ratio of the emission intensity of 387 nm to that of 421 nm is plotted against volume percentage of precursor in Fig. 9. As the volume percentage increases, the excitonic emission at 387 nm, gets decreased compared to the surface state emission at 421 nm.

Normally we expect the relative intensity of surface states to increase as the particle size decreases. However E. Hanamura [27] showed that there will be increase in oscillator strength with the decrease in particle size, so that there is an overall decrease in relative intensity of surface state emission. In the present case, beyond 1.4 %volume concentration, we infer the oscillator strength gets stabilized sot that the relative intensity shows a reverse trend. However at this concentration the particle size distribution also gets affected as seen from the broader nature of the emission spectrum.

Comparing the emissions of colloidal TiO_2 nanoparticles, it is clear that the size reduction of particles actually makes an impact on the fluorescence emission. Annealing the colloidal nanoparticles can cause aggregation and hence defect densities from grain boundaries. Thus confinement effects and also the increased surface states at nano regime play a vital role in the fluorescence emission of colloidal and annealed TiO_2 nanoparticles.

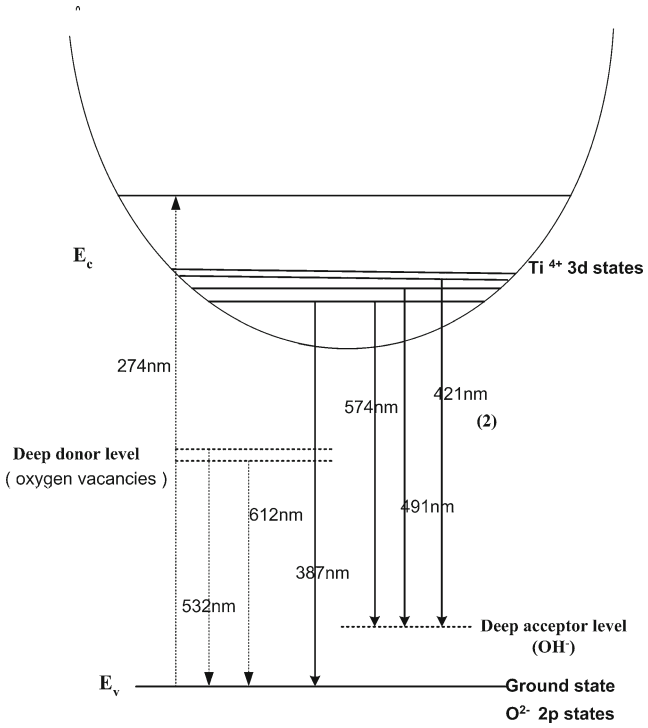

Fig. 8 Emission mechanism for TiO_2 nanoparticles

Conclusions

TiO_2 nanoparticle colloids were prepared by hydrothermal method. The optical absorption study shows a blue shift of absorption edge, indicating quantum confinement effect. The X-ray diffraction studies show that the colloidal nanoparticles are almost in anatase phase with a particle size of around 7 nm and annealed nanocrystals are of size around 14 nm. The Transmission electron micrographs (HRTEM) colloidal nanoparticles shows that the particles are having

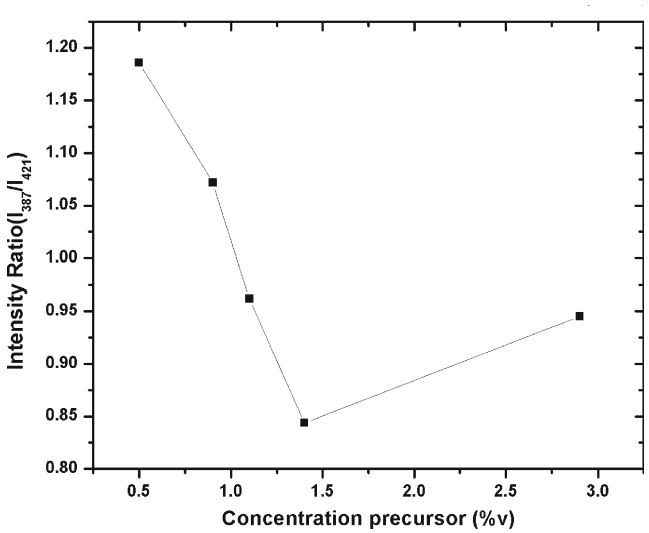

Fig. 9 Intensity ratio of excitonic and dominant surface state emissions

spherical shape and the size of the particles is found out to be around 2.5 nm. The large spectral range investigated allows observing simultaneously direct and indirect band gap optical recombination. The emission studies carried out show four peaks, which are found to be generated from excitonic as well as surface state transitions. It is found that the emission wavelengths of these colloidal nanoparticles and annealed nanoparticles show two category of surface state emission in addition to the excitonic emission.

Acknowledgments The authors wish to acknowledge UGC New Delhi for the financial assistance through CELOS project.

References

1. Li L, Hu J, Yang W, Alivisatos AP (2001) Nano Lett 1(7):349–351
2. Alivisatos AP (1996) Science 271:933–937
3. Singh Nalwa H (2000) Nanostructured materials and nanotechnology. Academic Press 257–259
4. Wang Y, Herron N (1988) J Phys Chem 92:4988
5. Brus LE (1983) J Chem Phys 79:5566
6. Ito S, Yamada Y, Kuze M, Tabata K, Yashima T J Mater Sci 39 (18):5853–5856
7. Nakato Y, Tsumura A, Tsubomura H (1982) Chem Phys Lett 85:387
8. Oregan B, Gratzel M (1991) Nature 353:737
9. Berenson ME (1984) Color Res Appl 9(2):98–102
10. Hudec B, Husekova K, Dobrocka E, Lalinsky T, Aarik J, Aidla A, Frohlich K (2010) IOP Conf Series Mater Sci Eng 8:012024
11. Zhang JZ (2000) J Phys Chem B 104(31):7239–7253
12. Plugaru R, Cremades A, Piqueras J (2004) J Phys Condens Matter 16:S261–S268
13. Pascual J, Camassel J, Mathieu H (1978) Phys Rev B 18:5606–5614
14. Glassford KM, Chelikowsky JR (1992) Phys Rev B 45:3874–3877
15. Serpone N, Lawless D, Khairutdinov R (1995) J Phys Chem 99:16646
16. Shirke BS, Korake PV, Hankare PP, Bamane SR, Garadkar KM J Mater Sci Mater Electron. doi:10.1007/s10854-010-0218-4
17. Tang H, Berger H, Schmid PE, Levy F (1993) Solid State Commun 87(9):847–850
18. Zhao Y, Li C, Liu X, Feng Gu, Jiang H, Shao W, Zhang L, He Y (2007) Mater Lett 61:79–83
19. Wang X, Feng Z, Shi J, Jia G, Shen S, Zhou J, Li C (2010) Phys Chem 12:7083–7090
20. Koch U, Fojtik A, Weller H, Henglein A (1985) Chem Phys Lett 122:507
21. Irimpan L, Deepthy A, Krishnan B, Nampoori VPN, Radhakrishnan P (2007) Size dependent fluorescence spectroscopy of nanocolloids of ZnO. J Appl Phys 102:063524
22. Jacques I (1971) Pankove - *Optical processes* in *semiconductors.* 422 pages –
23. Daude N, Gout C, Jouanin C (1977) Phys Rev B 15:3229
24. Madhu Kumar P, Badrinarayanan S, Sastry M (2000) Thin Solid Films 358:122–130
25. Mochizuki S (2003) Physica B 340–342:944–948
26. Pan D, Zhao N, Wang Q, Jiang S, Ji X, An L (2005) Adv Mater 17:1991
27. Hanamura E (1990) Phys Rev B 42:1724